1   **Chondrites as samples of differentiated planetesimals**

2

3   Linda T. Elkins-Tanton, Benjamin P. Weiss, and Maria T. Zuber

4

5   *Department of Earth, Atmospheric, and Planetary Sciences, Massachusetts Institute of*

6   *Technology, Cambridge, MA, USA, ltelkins@mit.edu, bpweiss@mit.edu, zuber@mit.edu.*

7

8   *Corresponding author: Linda T. Elkins-Tanton, Department of Earth, Atmospheric, and*

9   *Planetary Sciences, Massachusetts Institute of Technology, Cambridge, MA, USA, 02139,*

10   *ph: 617-253-1902*

11   *Email: ltelkins@mit.edu*

12

1 ABSTRACT

2 **Chondritic meteorites are unmelted and variably metamorphosed aggregates of**

3 **the earliest solids of the solar system. The variety of metamorphic textures in**

4 **chondrites motivated the "onion shell" model in which chondrites originated at**

5 **varying depths within a parent body heated primarily by the short-lived**

6 **radioisotope ^{26}Al, with the highest metamorphic grade originating nearest the**

7 **center. Allende and a few other chondrites possess a unidirectional magnetization**

8 **that can be best explained by a core dynamo on their parent body, indicating**

9 **internal melting and differentiation. Here we show that a parent body that accreted**

10 **to >~200 km in radius by ~1.5 Ma after the formation of calcium-aluminum-rich**

11 **inclusions (CAIs) would have a differentiated interior, and ongoing accretion would**

12 **add a solid undifferentiated crust overlying a differentiated interior, consistent with**

13 **formational and evolutionary constraints inferred for the CV parent body. This**

14 **body could have produced a magnetic field lasting more than 10 Ma. This**

15 **hypothesis represents a new model for the origin of some chondrites, presenting**

16 **them as the unprocessed crusts of internally differentiated early planetesimals. Such**

17 **bodies may exist in the asteroid belt today; the shapes and masses of the two largest**

18 **asteroids, 1 Ceres and 2 Pallas, can be consistent with differentiated interiors,**

19 **conceivably with small iron cores with hydrated silicate or ice-silicate mantles,**

20 **covered with undifferentiated crusts.**

1. INTRODUCTION

2   The antiquity and abundance of CAIs in CV chondrites have long suggested an early

3   parent body accretion age. New Pb-Pb and Al-Mg ages of chondrules in CVs indicate

4   they may be among the oldest known in any chondrite class, with ages ranging from ~0

5   to ~3 Ma after CAIs (Amelin and Krot 2007, Connelly et al. 2008, Hutcheon et al. 2009)

6   (Fig. 1). The time of accretion of a body controls the amount of initial ^{26}Al, which was

7   likely uniformly distributed in the inner protoplanetary disk (Jacobsen et al. 2008).

8   Bodies that accreted to more than ~20 km radius before ~1.5 Ma after the formation of

9   CAIs likely contained sufficient ^{26}Al to melt internally from radiogenic heating (Hevey

10   and Sanders 2006, Merk et al. 2002, Sahijpal et al. 2007, Urey 1955). These early-

11   accreting bodies would have melted from the interior outward, resulting in an interior

12   magma ocean under a solid, conductive, undifferentiated shell (Ghosh and McSween Jr.

13   1998, Hevey and Sanders 2006, McCoy et al. 2006, Merk et al. 2002, Sahijpal et al. 2007,

14   Schölling and Breuer 2009). This shell would consist of the same chondritic material that

15   made up the bulk accreting body before melting began; further, and critically, ongoing

16   accretion would add undifferentiated material to the crust, and this material may even

17   have bulk compositions distinct from the differentiated interior.

18   Allende and a few other chondrites possess a unidirectional magnetization (Blum et

19   al. 1989, Wasilewski 1981, Weiss et al. 2010). Funaki and Wasilewski (1999) suggested a

20   liquid metallic core dynamo origin for magnetism on the CV parent body. Weiss et al.

21   (2010) described how unidirectional magnetization in Allende is consistent with a field

22   lasting >10 Ma. The variety of metamorphic textures in chondrites originally motivated

23   the "onion shell" model in which chondrites originated at varying depths within a parent

1   body heated primarily by the short-lived radioisotope ^{26}Al, with the highest metamorphic

2   grade originating nearest the center (Miyamoto et al. 1981, Taylor et al. 1987). Now, the

3   metamorphic, magnetic, and exposure age data collectively indicate a new model for the

4   CV chondrite parent body in which interior melting is incomplete and a magma ocean

5   remains capped by an undifferentiated chondritic shell. This conductive lid insulates the

6   internal magma ocean, slowing its cooling and solidification by orders of magnitude

7   while still allowing sufficient heat flux out of the core to produce a dynamo with

8   intensities consistent with magnetization in Allende [see analysis in (Weiss et al. 2008)].

9   Materials in the undifferentiated lid experienced varying metamorphic conditions.

10   Chondritic meteorite samples, including Allende, provide motivation for this study.

11   We seek to define the accretion age and size that would allow internal differentiation of a

12   body consistent with Allende originating in the unmelted crust. A chondritic surface, a

13   silicate or ice-silicate mantle and crust, and an iron core should characterize such a body.

14   Further, we will investigate the implications of internally differentiated bodies, including

15   their possible existence in the asteroid belt today. This study is designed to test the

16   feasibility of internal differentiation with a retained primitive crust, and the feasibility of

17   generating a long-lived magnetic core dynamo on such a body.

18

19   2. MODELS AND METHODS

20   To calculate heat fluxes, the possibility of a core dynamo, and temperature gradients

21   in the unmelted crust, we assume instantaneous accretion and solve the heat conduction

22   in a sphere with initial ^{26}Al evenly distributed (Hevey and Sanders 2006). The body is

23   heated homogeneously but radiates energy into space, producing a hot interior and chilled

1   crust. If the interior exceeds its solidus temperature sufficiently, the resulting interior

2   magma ocean would advect heat to the base of the crust, where heat transfer continues

3   through the far slower process of conduction.

4   Although new models and observations indicate rapid accretion (Johansen et al.

5   2007), the accretion of planetesimals early in solar system history was certainly not

6   instantaneous, as discussed in Ghosh et al. (2003), Merk et al. (2002), and Sahijpal et al.

7   (2007). A hypothetical parent body with 300-km radius receives $\sim 10^{25}$ J in kinetic energy

8   during incremental accretion, sufficient to heat the body homogeneously by only 10 to

9   20°C (see SD). Thus the first-order temperature driver prior to 2 Ma after CAIs was ^{26}Al

10   heating. The complexity and stochastic nature of boundary conditions, sizes and rates of

11   impactors, and energy partitioning during incremental accretion also means that

12   incremental model results are necessarily non-unique. Incremental accretion models are

13   likely therefore to require a Monte Carlo approach. Because our intention is to

14   demonstrate the feasibility of partial differentiation rather to model it explicitly, we

15   conclude that instantaneous accretion is a reasonable simplification for calculating core

16   heat flux.

17   Incremental accretion, though it may not influence the heating of the body, does

18   partially control cooling. A thickening conductive undifferentiated lid added to an

19   initially partially melted planetesimal will slow its heat flux into space and therefore

20   lessen the driving mechanism for a magnetic core dynamo. A simple model of

21   incremental accretion is considered in comparison to the instantaneous models; this

22   model is described below.

23   **2.1 Heating and heat transfer**

1   The initial [26]Al content of CV chondrites is a controlling parameter in these

2   calculations.   Kunihiro et al. (2004) find that there is insufficient radiogenic aluminum in

3   CO chondrites to cause more than minimal melting even with the help of radiogenic [60]Fe,

4   and also argue that the CV parent body was unlikely to have melted. However, their

5   conclusion for CV chondrites is based on an initial [26]Al content identical to that of CO

6   chondrites and instantaneous accretion. Here we find that the potentially older age of CV

7   chondrules (the youngest being up to 1 Ma older than those in CO chondrites) combined

8   with non-instantaneous accretion mean the CV body could have melted. See Table 1 for

9   model parameters including bulk aluminum content.

10   Following Hevey and Sanders (2006) we assume instantaneous accretion and solve

11   the heat conduction in a sphere with initial [26]Al evenly distributed:

12    $$\rho C_P \frac{\partial T}{\partial t} = \frac{1}{r^2}\frac{\partial}{\partial r}\left(kr^2\frac{\partial T}{\partial r}\right) + A_0(r,t),$$ (1)

13   where ρ is density, C_p is the heat capacity of the chondrite, T is temperature, t is time, r is

14   radius, k is thermal conductivity, and A_0 is the radiogenic heat source per volume per

15   time. The temperature profile in these planetesimal models is initially calculated using an

16   analytic solution as given by Carslaw and Jäger (1946) and Hevey and Sanders (2006):

17

18    $$T = T_0 + \frac{\kappa A_0}{K\lambda}e^{-\lambda t}\left[\frac{R\sin\left(r\left(\frac{\lambda}{\kappa}\right)^{\frac{1}{2}}\right)}{r\sin\left(R\left(\frac{\lambda}{\kappa}\right)^{\frac{1}{2}}\right)} - 1\right] + \frac{2R^3 A_0}{r\pi^3 K}\sum_{n=1}^{\infty}\frac{-1^n}{n\left(n^2 - \frac{\lambda R^2}{\kappa\pi^2}\right)}\sin\left(\frac{n\pi r}{R}\right)e^{-\frac{\kappa n^2 \pi^2 t}{R^2}}$$ (2)

1   where the variables are as defined in Table 1, and t is the time elapsed since accretion.

2   The power from ^{26}Al, A_0 in W m^{-3}, is obtained by multiplying the decay energy of

3   aluminum, converted to J kg^{-1}, with the aluminum content of chondrites, the ^{26}Al decay

4   constant, the material density, and the initial ^{26}Al/^{27}Al ratio, and similarly for the other

5   radioactive nuclides considered (see Supplementary Data, SD). To obtain the initial

6   power for later accretion times, the initial A_0 is multiplied by $e^{-\lambda t}$, where t is here the

7   instantaneous time of accretion.

8   The accreted chondritic material is assumed to begin to melt at 1,200°C and reach its

9   liquidus at 1,600°C at the low but non-zero pressures of the planetesimal interiors (in a

10   Vesta-sized body the pressure at the bottom of a mantle magma ocean will be 1 kb or less,

11   and over that pressure range the solidus will change by less than 20°C and the adiabat by

12   less than 4°C). These temperatures are based on experimental melting of Allende bulk

13   compositions (Agee et al. 1995) taking into consideration the absence of the iron metal

14   component (removed to the core) and the loss of some volatiles. Melting is calculated

15   using the following simplified expression for melt production per degree above the

16   solidus:

17        $$f = \Delta T \frac{df}{dT} = \Delta T \frac{C_P}{H_f} = (0.002)\Delta T \quad \text{[fraction by weight]},\tag{3}$$

18   where C_p and H_f are the heat capacity and heat of fusion of the silicates, and ΔT is the

19   temperature excess of the melt source beyond its solidus (Hess, 1992). The coefficient

20   0.002 therefore has units of K^{-1} and the resulting f is a nondimensional weight fraction.

1   Latent heat of melting is similarly applied to the temperature of the melting material.

2   The total temperature change for complete melting in this simple linear melting scheme,

3   using values from Table 1, is

4        $$\Delta T = \frac{H_f}{C_P} \approx 500K \,.$$ (4)

5   The latent heat temperature change is applied to the melting material at each time step of

6   the model until complete melting is achieved. The model tolerates temperatures in the

7   magma ocean above the liquidus temperature, and conductive heat loss through the lid

8   continues. High temperatures lead to melting and thus thinning of the lid.

9   We calculate thermal profiles using equation 2 at intervals of 1,000 years until the

10   body has melted 10% by volume (so much radiogenic heat is created in these bodies that

11   the degree of melting is 100%, and volume here refers to a fraction of the total

12   planetesimal volume). After this point, the internal magma ocean is treated as a

13   homogeneous adiabatic fluid, and conduction of heat through the unmelted crust limits

14   the heat flux available to drive the core dynamo.

15   These calculations are done using a finite difference formulation of the heat

16   conduction equation in spherical coordinates for the conductive lid, which is defined as

17   the material at temperatures below 1,400°C based on an assumption that melting above

18   50% will produce a convecting fluid no longer constrained by a solid network of residual

19   crystals. In this simulation all material in the conductive lid is assumed to be porous,

20   unmelted chondritic material. Although the temperature profiles indicate areas of partial

21   melt and sintering, these are not treated in the calculations.

1   At each step the heating contributions of ^{235}U, ^{238}U, ^{232}Th, ^{40}K, and ^{26}Al are added,

2 assuming chondritic concentrations, to each element in the conductive lid and to the bulk

3 magma ocean beneath. Concentrations, heat production, and calculation schema for U,

4 Th, and K are from Turcotte and Schubert (2002); Al values and references are listed in

5 Table 1. Heating from ^{26}Al is given by

6       $$H(t) = H_0 C_0 e^{-\lambda t} \ [\text{W kg}^{-1}], \qquad\qquad\qquad (5)$$

7 where H_0 is heating rate of ^{26}Al, C_0 is the fraction of ^{26}Al in the bulk material, and λ is

8 the decay constant for ^{26}Al. For values and references see Table 1.

9   Radiogenic heat is added to the crust in proportion to the silicate portion of the bulk

10 chondrite, subtracting volume for pore space, assumed to be 25%, and for metal fraction,

11 and to the magma ocean, which is assumed to be 100% bulk silicate.

12   Heat is conducted upward from the magma ocean to the surface through the

13 conductive lid using the following expression for temperature controlled by heat

14 conduction in a sphere:

15    $$T_r^t = T_r^{t-dt} + \kappa dt \left(\frac{1}{r} dr \left(T_{r+dr}^{t-dt} - T_{r-dr}^{t-dt} \right) + \frac{1}{dr^2} \left(T_{r+dr}^{t-dt} - 2T_r^{t-dt} + T_{r-dr}^{t-dt} \right) \right) + dt \frac{H}{C_p}, \qquad (6)$$

16 where dt is a Courant time step determined by thermal diffusivity, and dr is the radial

17 length of an element in the finite difference grid that does not exceed 1 km. At each time

18 step the temperature at the bottom of the conductive lid is examined, and if the bottom of

19 the lid has melted, the radius of the bottom of the grid is adjusted upward and the grid

20 points redefined; latent heat is also considered at each melting step. If more melting has

21 occurred then the appropriate volume is added to the core, at the current temperature of

22 the magma ocean.

1   Although iron-nickel metal melts at temperatures below primitive silicate melting

2   temperatures, the metal liquid may be unable to segregate into a core until the silicates

3   are partially molten. Previous studies differ on whether core segregation occurs near

4   950°C, at the iron alloy eutectic, or in the range 1,170 to 1,570°C, between the solidus

5   and liquidus of the silicate portion [see Sahijpal et al. (2007) and references therein].

6   Here we assume metallic core formation occurs instantaneously when the bulk chondritic

7   material reaches its model solidus, 1,200°C. At the point that the body has reached 10%

8   melting by volume, the core is assumed to be at thermal equilibrium with the small

9   internal magma ocean from which it just segregated (for a 100-km radius body, at 10

10   vol% melting the internal convecting magma ocean reaches a radius of about 46 km, and

11   if the body began with 20 vol% metals the core has a radius of 30 km).

12   The core is assumed to contain no U, Th, K, or Al; all these elements are compatible

13   with the silicate magma ocean and not with the metallic core material. Thus the core,

14   initially at thermal equilibrium with the overlying magma ocean, has a thermal history

15   entirely driven first by the radiogenic heating of the overlying magma ocean (during

16   which the core is heated by the magma ocean, and heat flux is therefore into rather than

17   out of the core), and then by secular cooling of the body (during which the core cools and

18   heat moves back into the magma ocean).

19   To calculate these changes, at each time step heat flux through the core-mantle

20   boundary is calculated as

21   $$F_{core} = \kappa_{core} \rho_{core} C_{p,core} \frac{dT}{dr} \quad [\text{J m}^{-2} \text{ s}^{-1}], \tag{7}$$

22   and the resulting temperature change in the core is given as

1 $$\Delta T_{core} = \frac{3dtF_{core}}{\rho_{core}C_{P,core}r_{core}} \ [K],\tag{8}$$

2 which is a simplification in this geometry of the general statement

3 $$\Delta T = \frac{dtF_{core}A_{core\_surface}}{V_{core}\rho_{core}C_{P,core}}.\tag{9}$$

4 The corresponding temperature change in the magma ocean is given as

5 $$\Delta T_{MO} = \frac{3dtF_{core}r_{MO,top}^{2}}{\rho_{MO}C_{P,MO}\left(r_{MO,top}^{3} - r_{core}^{3}\right)} \ [K],\tag{10}$$

6

7 where $r_{MO,top}$ is the radius at the top of the internal magma ocean, equivalent to the radius

8 at the bottom of the conductive lid. Next, the heat flux out of the magma ocean and into

9 the conductive lid is calculated using an equivalent statement to equation 6, and the

10 corresponding additional temperature change in the magma ocean is calculated using an

11 equivalent statement to equation 9.

12 The physics and chemistry of cooling an internal magma ocean on a small body are

13 not well understood. Mineral phases solidifying from the magma ocean will be dense in

14 comparison to the magma ocean, with the exception of plagioclase feldspar. The time

15 required for mineral grains to either sink or float out of the convecting magma ocean is,

16 however, possibly longer than the time of solidification of the body (Elkins Tanton et al.

17 2008). We therefore assume for simplicity that the conductive lid does not significantly

18 thicken from beneath while the internal magma ocean is still convecting, as that would

19 require material to adhere to its bottom and leave the convecting magma ocean. Rather,

20 the magma ocean continues to convect and cool and fractionate under the existing

1   thinnest conductive lid. Convection is assumed to be inhibited at temperatures below

2   1,000°C by a high crystal fraction in liquids evolved through some degree of fractional

3   solidification. No latent heat of solidification is applied during cooling.

4   For the simple incremental accretion model shown here, the initial assumptions are

5   the same: A radius of instantaneous accretion is chosen and heating calculated until 10%

6   of the planetesimal's volume is melted. The calculations are then passed to the convective

7   code, with conduction occurring through the unmelted lid. Shells of cold undifferentiated

8   material are added to the outside of the planetesimal in increments of equal radius until a

9   final radius is acquired, in a simple approximation of the addition of new material to the

10   outside of the planetesimal. Thus, heat flux is inhibited through the growing lid. The new

11   material added to the exterior is assumed to have the same radioactive element

12   composition as the initial material.

13   **2.1 Calculating internal structure in asteroids**. To address whether examples of

14   differentiated parent bodies of the kind we propose are conceivably preserved in the

15   asteroid belt today, we consider the simple case of a rotating, hydrostatic figure

16   composed of a core and mantle, each of uniform density (Fig. SD2). For such a body it is

17   possible to relate shape, gravitational moments and internal structure. We invoke the

18   formalism of Dermott *(1979),* who derived a relationship between the moment of inertia

19   factor (C/Ma^2) and the internal density structure for a planetary body with this

20   configuration

$$\frac{C}{Ma^2} = \frac{2}{5}\left[\frac{\rho_m}{\langle\rho\rangle} + \left(1 - \frac{\rho_m}{\langle\rho\rangle}\left(\frac{r_c}{R}\right)^2\right)\right]$$

21   (11)

1 where M, R and $<\rho>$ represent the mass, radius and mean density of the body, C is the

2 moment about the polar axis, a is the semi-major equatorial axis, r_c is the core radius, and

3 ρ_m and ρ_c are the mantle and core densities. Introducing an expression for the mean

4 density

$$\langle \rho \rangle = \frac{\left(\frac{4}{3}\right)\pi\left[\rho_c r_c^3 + \rho_m\left(R^3 - r_c^3\right)\right]}{\left(\frac{4}{3}\right)\pi R^3}$$

5 (12)

6 allows the mantle and core densities to be expressed as

$$\rho_m = \langle \rho \rangle \left[\frac{\frac{5}{2}\frac{C}{Ma^2} - \left(\frac{r_c}{R}\right)^2}{1 - \left(\frac{r_c}{R}\right)^2}\right],$$

7 (13)

8 and

$$\rho_c = \frac{\langle \rho \rangle - \rho_m\left[1 - \left(\frac{r_c}{R}\right)^3\right]}{\left(\frac{r_c}{R}\right)^3}.$$

9 (14)

10   The consistency of internal structures with the hydrostatic assumption can also be

11 tested using an expression between hydrostatic flattening and moment of inertia factor

12 (Jeffreys 1959)

$$f_{hyd} = \frac{q}{1 + \left(\frac{25}{4}\right)\left[1 - \left(\frac{3}{2}\right)\frac{C}{Ma^2}\right]}$$

13 (15)

1   where

2    $$q = \frac{\omega^2 a^3}{GM} ,$$ (16)

3   and ω is the rotational angular velocity and G is the universal constant of gravitation.

4   On the basis of observations of shape, mass and surface composition inferred from

5   infrared spectra, we consider asteroids 1 Ceres and 2 Pallas as the likeliest candidates

6   among the largest asteroids for the proposed parent body and we investigate models of

7   their interior structures using the expressions above. Fig. SD3 plots expression (15)

8   combined with axial measurements in Table SD2, and verifies the validity of the

9   hydrostatic shape of both bodies within the bounds of measurement error.

10   These simple calculations are intended to demonstrate the plausibility of the present-

11   day existence of a differentiated CV chondrite parent body. Additional observations will

12   be required to test more rigorously whether either or both of these bodies (or others)

13   satisfy all required criteria.

14

15   3. RESULTS

16   If accreted before ~1.5 Ma after CAIs, the planetesimal melts from its interior

17   through radiogenic heat. In the largest body considered here, 500 km radius, an internal

18   magma ocean is still generated if the body accretes by 1.6 Ma after CAIs, but for smaller

19   bodies and at any later accretion times there is insufficient heat to produce an internal

20   magma ocean (Figure 2). This precise ending point of melting is dependent upon initial

21   parameters that might not be well constrained, including initial ^{26}Al content of the parent

22   body and thermal diffusivity of the variably porous and sintered conductive lid.

1   Calculation of core heat flux is a necessary first step to determining the possibility of

2   a core dynamo. Here the rapid heat transfer of convection in a liquid internal magma

3   ocean maximizes core heat flux. The magma ocean rapidly heats beyond the temperature

4   of the non-radioactive core, so initial heat flux across the core-mantle boundary transfers

5   heat into the core, rather than out. All bodies considered here reach their peak magma

6   ocean temperatures within 5 Ma after CAI formation (Figures 3, 4). Shortly after

7   radiogenic heating peaks and the body begins secular cooling heat flux from the core

8   becomes positive, compatible with creating a core dynamo.

9   All bodies considered here have sufficient size to produce a core dynamo. Bodies

10   larger than ~100 to 150 km radius will produce a core dynamo lasting longer than 10 Ma,

11   and those larger than ~300 to 350 km radius will produce a core dynamo lasting longer

12   than 50 Ma (Figure 3). The volume fraction of metal in the bulk material determines the

13   size of the core, but over the range of metal fractions considered here (0.05 to 0.2), core

14   heat flux and thus magnetic dynamo are not greatly affected (Figure 4).

15   As shown by Hevey and Sanders (2006), these early-accreting planetesimals melt

16   extensively and retain only a very thin crust. In the instantaneous accretion convective

17   models used here the crust is artificially limited to a thickness no less than 2% of the

18   body's radius (Figure 5). Only in bodies accreting later than ~1.3 Ma are thicker crusts

19   naturally retained on the bodies; radiogenic heating is lower and so less of the

20   planetesimal's shell melts. The thermal gradient within the stable undifferentiated crust,

21   from liquid silicate temperatures at its bottom boundary to space equilibrium blackbody

22   temperatures at its surface (Hevey and Sanders 2006, Sahijpal et al. 2007), would

23   produce regions of varying metamorphic grade.

1   The simple incremental accretion models, in which the initially instantaneous core

2   then receives increments of cold material to its surface over an additional 1 to 2 Myr,

3   would also produce core dynamos. The thickening cold crust inhibits heat flux out of the

4   body and so lessens core heat flux but also lengthens the period of internal convection

5   (Figure 3). Determining the combinations of rate of accretion and final body size that

6   allow or disallow magnetic dynamos is beyond the scope of this project, but these initial

7   studies indicate that dynamos can be lengthened by adding insulating crust, and that very

8   thick added crusts would inhibit dynamos.

9   Asteroid 1 Ceres displays a hydrostatically relaxed shape from which its internal

10   structure has previously been modelled (Castillo-Rogez and McCord 2010, Thomas et al.

11   2005). And a recent analysis of the shape of 2 Pallas (Schmidt et al. 2009) finds a close

12   fit of the shape to a hydrostatically relaxed spheroid. Given current knowledge of shape,

13   Ceres is most consistent with a differentiated interior, as previously noted (Thomas et al.

14   2005), but both undifferentiated and differentiated interiors are permissible for Pallas.

15   An assumed iron core of $\rho_c \sim 7800$ kg m^{-3} in 1 Ceres constrains the core to radius to

16   $0.22 < r_c/R < 0.5$ and limits mantle density to $1000 < \rho_m < 1950$ kg m^{-3} (Figure 6). For

17   Pallas, assumption of an iron core, again with density ρ_c-7800 kg m^{-3} yields a range of

18   fractional core size of $0.3 < r_c/R < 0.6$ and constrains the mantle density to $1000 < \rho_m <$

19   2300 kg m^{-3} (Figure 6). A mantle density of 1,000 kg m^{-3} implies pure water ice, while

20   higher values likely indicate mixed ices and silicates.

21

22   4. DISCUSSION

23   **4.1 Core dynamos on planetesimals**

1   These core dynamo calculations have several caveats. Heat flux through the

2   undifferentiated crust may be enhanced by fluid flow (Young et al. 2003) or slowed by a

3   porous low-conductivity crust (Haack et al. 1990). If a body 250 km or more in radius

4   accretes as late as ~2.0 Ma after CAIs, its internal temperature reaches ~1,000°C and it

5   may form a core, but its silicate mantle will not melt more than a small fraction;

6   compositional convection in the core would then likely be necessary for dynamo

7   generation (Nimmo 2009). Therefore, ~2.0 Ma is the latest limit on accretion that will

8   allow a core dynamo using the parameters chosen in these models. The upper time limit

9   is sensitive to choice of heat capacity, final body radius, ^{26}Al and ^{60}Fe content, and

10   thermal boundary conditions and has uncertainties of ~±1 Ma.

11   Throughout most of the parameter space explored here bodies would create dynamos

12   lasting tens of millions of years (Figure 2). Our code halts calculation when the magma

13   ocean is assumed to end convection, but even conductive heat flux may be sufficient to

14   drive dynamos in some cases. Sufficient heat flux for a core dynamo is a pervasive and

15   robust outcome in these models. Although convection is a necessary but not sufficient

16   criterion for dynamo action, it appears feasible that planetesimals also had other

17   properties (core size, core convective velocity, spin rate) suitable for dynamo generation

18   (Weiss et al. 2008, Weiss et al. 2010).

19   **4.2 The growing crust of a planetesimal**

20   The body must retain or acquire a sufficiently thick crust to both create radial source

21   zones for each chondrite type and to be stable against foundering. Metasomatism of

22   Allende likely began within 1 Ma after CAI formation (Hohenberg et al. 2004,

23   Pravdivtseva et al. 2003), as water was mobilized within the planetesimal. The presence

of talc and the absence of serpentine indicate peak temperatures of ~300-350°C (Brearley

1997, Krot et al. 1995), while organic thermometry and presolar gases in nanodiamonds

place an upper limit of <~600 °C (Cody et al. 2008).

Figure 7 contains a compendium of data constraining the timing of events on the CV

parent body and on other early-accreting bodies. Although all the isotopic systems

included in this table do not have equivalent precision and accuracy, in aggregate they

provide a sufficiently clear timeline to guide the modelling efforts presented in this paper.

Specifically, the CV parent body contains chondrules not younger than about 3 Ma after

first CAIs. The majority, and perhaps all, CAIs and chondrules in the CV parent body are

older than these limits.

Metamorphism of chondrite parent bodies appears to stretch for tens of millions of

years, though peak temperatures for the CV parent body were reached at 5 to 10 Ma after

CAIs, based on I-Xe chronometry for Allende (Swindle 1998). These ages are within

error of the 5-10 Ma ages Mn/Cr ages for CV fayalites, although no Mn/Cr ages have

actually been reported for Allende itself (Nyquist et al. 2009). These chronometric

systems are subject to uncertainties associated with the initial abundances of the parent

nuclides, their closure temperatures, and the homogeneity of their spatial distribution in

the solar system.

These constraints require that the planetesimal have a reasonably thick crust while

simultaneously producing a core dynamo. Instantaneous accretion models that consider

convective heat transfer produce crusts that are too thin to be stable against eruption and

impact foundering, and which have thermal profiles too steep to produce a sufficiently

1   large volume consistent with Allende's constraints. These thin crusts are also too old;

2   younger chondrules in Allende require ongoing accretion.

3   Planetesimals would be expected to continue accreting mass after the processes

4   proposed here are underway. Thus, colder material with younger chondrules would be

5   added after the majority of the body is accreted, and these younger chondrules would be

6   preferentially placed in near-surface material such as that hypothesized for the Allende

7   source. This initially cold crust will also yield significant metamorphosing but not

8   melting regions consistent with Allende's thermal constraints, over a body still producing

9   a core dynamo (Figure 2).

10   The fraction of ice in the planetesimal also affects the energy required to heat and

11   melt the silicate fraction of the body (Gilmour and Middleton 2009). Both accretionary

12   and radiogenic heat can be applied to melting (and possibly to evaporating) water before

13   silicate melting begins. Further, accretion of some icy material with the rocky chondritic

14   material would significantly enhance crustal formation through the cooling effect of

15   latent heat of melting. The accretion and differentiation of planetesimals that include both

16   ice and rock is pertinent for not just production of chondrites, but also possibly for

17   production of Pallas and Ceres.

18   **4.3 Densities of solids and liquids and likelihood of eruption**

19   Magma is unlikely to rise through the undifferentiated lid of the planetesimal.

20   Basaltic or picritic magmas would cool and solidify as they rise into the cool crust,

21   limiting their radius of maximum rise. Additionally, buoyancy alone is unlikely to drive

22   silicate eruption in small bodies with cool crusts. Because of the porous nature of

23   unheated chondrites, molten Allende liquids are in many cases denser than the

1   undifferentiated planetesimal lid (Figure 8). On Earth, Mars, and the Moon, gravity

2   forces buoyant magmas to erupt, while denser magmas may be erupted through volatile

3   pressure. Wilson and Keil (1997) predict fire-fountaining lava eruptions on Vesta driven

4   by volatiles in magmas, but in our models we predict that the magmas will be largely dry.

5   On early-forming planetesimals gradual heating would drive off volatiles before silicate

6   melting begins [this is in contrast to Earth, where volatiles are either introduced to the

7   silicate solids and trigger melting by their presence (Sisson and Grove 1993) or they exist

8   in equilibrium with near-solidus silicates]. We therefore conclude that only from the

9   hottest bodies with the thinnest crusts will basaltic magmas erupt, or in cases where

10   volatiles were not driven off before magma genesis, will basaltic magmas erupt. The

11   conductive transfer and convection modelled here accounts for the effects of melting

12   from below.

13   We postulate that the picritic to basaltic silicate magma ocean liquids in the interior

14   magma oceans of these planetesimals will not fully infiltrate and cover the

15   undifferentiated crust of these bodies. Crustal stability in this case relies on three

16   processes: buoyancy of the crust, slow erosion from its bottom, and thickness sufficient

17   to prevent impacts from breaching the crust.

18   Because of the porous nature of unheated chondrites, molten Allende liquids (red

19   line in Fig. 8) are in many cases denser than the undifferentiated, unsintered, planetesimal

20   lid (grey range in Fig. 8) but close to the density of sintered material. In Fig. 8, the

21   Allende liquid densities are calculated from experimental compositions given in Agee et

22   al. (1995), using partial molar volumes and techniques from Kress and Carmichael (1991)

23   and Lange and Carmichael (1987); also see previous applications of this technique in

1   Elkins-Tanton et al. (2003). All measurements and calculations are done at 1 bar and

2   room temperature. Here, as on the Moon, magmas would require a significant impact

3   basin to erupt onto the surface through the more buoyant crust.

4   On such a small body viscous traction of the convecting magma ocean liquids on the

5   bottom of the lid will be minimal; not only do magma ocean liquids have low viscosity,

6   but also the small gravitational fields make convective velocities commensurately small.

7   Erosion of the bottom of the crust through liquid convection is therefore negligible.

8   Finally, the crust must be thick enough to prevent the majority of impacts from

9   breaching it. The small gravity fields of planetesimals prevent very great impact crater

10 depths. Taylor et al. (1987) estimate that the maximum excavation depth expected on a

11 planetesimal with 500 km diameter is 20 km. Although simple heat transfer in our models

12 produces a thin crust, later accreting material is expected to produce a far thicker crust.

13 We therefore suggest that the average impact will disrupt but not breach the crust and that

14 in most cases impacts will not allow magma to erupt. We conclude that undifferentiated

15 chondritic crusts may successfully persist through the internal magma ocean stage,

16 particularly when the bodies accreted throughout and after the window available for

17 internal heating.

18 **4.4 Source regions for meteorite types in an internally differentiated**

19 **planetesimal**

20   At temperatures above ~430°C (Yomogida and Matsui 1984) the porous chondritic

21 material would sinter into a denser and stronger solid. At about the same temperatures,

22 fluids may be released from the *in situ* chondritic materials. Hydrous, briney, sulfidic, or

23 carbon-rich fluids will be able to rise efficiently through the chondritic crust at Darcy

1 velocities of meters to kilometers per year (Haack et al. 1990, Young et al. 2003). These

2 fluids may to quickly escape into space (Young et al. 2003). Even in the case where a

3 frozen ice crust slows escape, periodic impacts will disrupt this surface and aid escape.

4 Hydrous fluids are therefore not expected to pervasively or homogeneously metasomatize

5 the entire planetesimal crust. We note further that briney fluids are insufficient to create a

6 core dynamo: circulating saltwater of composition like Earth's seawater has electrical

7 conductivity more than four orders of magnitude less than iron-liquid metal [see

8 discussion in Schubert et al. (1996)].

9 The added cooler material accreting to the top of the crust will experience varying

10 degrees of thermal and fluid metamorphism, depending on its depth and time of

11 accretion. Some late-accreting material will be added after the main pulse of heating and

12 metasomatism, and so will not experience the same intensity of metamorphism. The

13 stochastic nature of crustal additions implies that metamorphic grade and cooling rate

14 may not be correlated in samples from the crust.

15 These models indicate that dynamos will operate on these bodies for tens of millions

16 of years, allowing a range of accreted crustal conditions to pertain. Only the deepest parts

17 of the crust will be infiltrated by silicate magmas. These events appear to correspond well

18 with the metasomatic and metamorphic events experienced by the CV chondrites, and

19 help to explain why CV chondrites almost never contain fragments of volcanic rock.

20 The least metamorphosed, brecciated, and reduced CV chondrites containing a

21 solar wind component, such as Vigarano and Mokoia, may have originated nearest the

22 surface. Beneath were the Bali-type oxidized CV chondrites, and at greater depth, the

23 Allende-type oxidized CV chondrites (Fig. 1). Rocks like the metachondrite NWA 3133

1   may have originated at greatest depth in the undifferentiated crust, while the few higher

2   petrologic-grade clasts found in Mokoia (Krot et al. 1998) may be rare samples of the

3   highly thermally metamorphosed lower crust (Fig. 1). Irons like Bocaiuva (Irving et al.

4   2004) may have come from the core-mantle boundary region of this same body (Fig. 1).

5   Further, Greenwood et al. (2010) argue that CK and CV chondrites may have formed on

6   the same parent body, with CK chondrites simply being more highly metamorphosed, and

7   therefore, deeper samples.

8   **4.5 The existence of internally differentiated planetesimals today**

9   Because of the limited lifetime of ^{26}Al and the longer apparent period over which

10   chondrite parent bodies were forming, many parent bodies likely heated without

11   significant melting. Bodies that formed before ~1 Ma likely melted sufficiently to

12   produce only a fragile crust, and may have developed into bodies with igneous surfaces

13   like Vesta, while those accreting more slowly would have obtained an internal magma

14   ocean and a thicker, metamorphosed but unmelted crust.

15   The shapes and masses of the two largest asteroids, 1 Ceres and 2 Pallas, can be

16   consistent with differentiated interiors, conceivably with small iron cores with hydrated

17   silicate or ice-silicate mantles. The range of mantle density permits ice-silicate

18   compositions, though in this scenario for 1 Ceres the mantle is ice-rich (perhaps >50 wt%

19   if there is no porosity, possibly not compatible with large-scale melting). The

20   corresponding range of mantle density for 2 Pallas permits more silicate-rich

21   compositions than Ceres.

22   Thus the asteroid melt may contain several examples of early-accreting bodies that

23   are internally differentiated. Unlike Vesta, Ceres and Pallas may retain their primitive

1 crusts over a differentiated interior. This is the central concept of this paper: That early

2 radiogenic of planetesimals can create partially differentiated bodies with undifferentiated

3 crusts, and that these bodies may have experienced magnetic core dynamos, varying

4 degrees of crustal metamorphism or magmatic intrusion, and that some partially

5 differentiated bodies may have persisted to the current day.

6

7   5. CONCLUSIONS

8   Planetesimals that largely accreted before ~1.5 Ma after CAIs are likely to

9 differentiate internally through radiogenic heating (Ghosh and McSween Jr. 1998, Hevey

10 and Sanders 2006, Sahijpal et al. 2007, Urey 1955). Most of these bodies are capable of

11 producing a core dynamo. The earliest-accreting bodies are likely to obtain igneous crusts

12 through foundering of their thin lids, but bodies that continue to accrete past ~1.5 Ma are

13 likely to have an undifferentiated crust not covered by basalt.

14   Bodies that are internally differentiated in the manner described here, therefore, may

15 well exist undetected in the asteroid belt. Other asteroids may have lost their hydrostatic

16 shapes through later impacts, and their surfaces may never have been covered with

17 erupted basalt; surfaces of these bodies may have remained chondritic throughout this

18 process. Such surfaces will therefore be composed of irregular, space-weathered

19 primitive material, perhaps with highly altered or even differentiated material at the

20 bottoms of the largest craters and in crater ejecta. This scenario can help explain the

21 mismatch between the enormous diversity (> 130) of parent bodies represented by

22 achondrites and the paucity (< 10) of basalt-covered asteroids.

23

7

References

C.B. Agee, J. Li, M.C. Shannon, S. Circone, Pressure-temperature phase diagram for the Allende meteorite, Journal of Geophysical Research 100(1995) 17725-17740.

Y. Amelin, A.N. Krot, Pb isotopic age of the Allende chondrules, Meteoritics and Planetary Science 42(2007) 1321-1335.

K.S. Bartels, T.L. Grove, High-pressure experiments on magnesian eucrite compositions - constraints on magmatic processes in the eucrite parent body, Proceedings of the Lunar and Planetary Science Conference 21(1991) 351-365.

J.D. Blum, G.J. Wasserburg, I.D. Hutcheon, J.R. Beckett, E.M. Stolper, Origin of opaque assemblages in C3V meteorites - implications for nebular and planetary processes, Geochemica et Cosmochimica Acta 53(1989) 543-556.

A. Brearley, Disordered biopyriboles, amphibole, and talc in the Allende meteorite: products of nebular or parent body aqueous alteration?, Science 276(1997) 1103.

D.T. Britt, S.J. Consolmagno, Stony meteorite porosities and densitied: A review of the data through 2001, Meteoritics and Planetary Science 38(2003) 1161-1180.

H.S. Carslaw, J.C. Jaeger, Conduction of Heat in Solids, Oxford Univesity Press, Oxford, 1946, 510 pp.

J. Castillo-Rogez, T.V. Johnson, M.H. Lee, N.J. Turner, D.L. Matson, J. Lunine, [26]Al decay: Heat production and a revised age for Iapetus, Icarus 204(2009) 658-662.

J. Castillo-Rogez, T.B. McCord, Ceres' evolution and present state constrained by shape data, Icarus 205(2010) 443-459.

G.D. Cody, C.M.O.D. Alexander, H. Yabuta, A.L.D. Kilcoyne, T. Araki, H. Ade, P. Dera, M. Fogel, B. Militzer, B.O. Mysen, Organic thermometry for chondritic parent bodies, Earth and Planetary Science Letters 272(2008) 446-455.

J. Connelly, Y. Amelin, A. Krot, M. Bizzarro, Chronology of the Solar System's Oldest Solids, The Astrophysical Journal Letters 675(2008) 121-124.

S.F. Dermott, Shapes and gravitational moments of satellites and asteroids, Icarus 37(1979) 575-586.

L.T. Elkins Tanton, E. Maroon, M.J. Krawczynski, T.L. Grove, Magma ocean solidification processes on Vesta, Lunar and Planetary Sciences Conference 39, Houston, TX, 2008.

L.T. Elkins-Tanton, E.M. Parmentier, P.C. Hess, Magma ocean fractional crystallization and cumulate overturn in terrestrial planets: Implications for Mars, Meteoritics & Planetary Science 38(2003) 1753-1771.

O.B. Fabrichnaya, The phase relations in the FeO-MgO-Al2O3-SiO2 system: An assessment of thermodynamic properties and phase equilibria at pressures up to 30 GPa, Calphad 23(1999) 19-67.

M. Funaki, P. Wasilewski, A Relation of Magnetization and Sulphidation in the Parent Body of Allende (CV3) Carbonaceous Chondrite, Meteoritics and Planetary Science 34(1999) A39.

A. Ghosh, H.Y. McSween Jr., A thermal model for the differentiation of Asteroid 4 Vesta, based on radiogenic heating, Icarus 134(1998) 187-206.
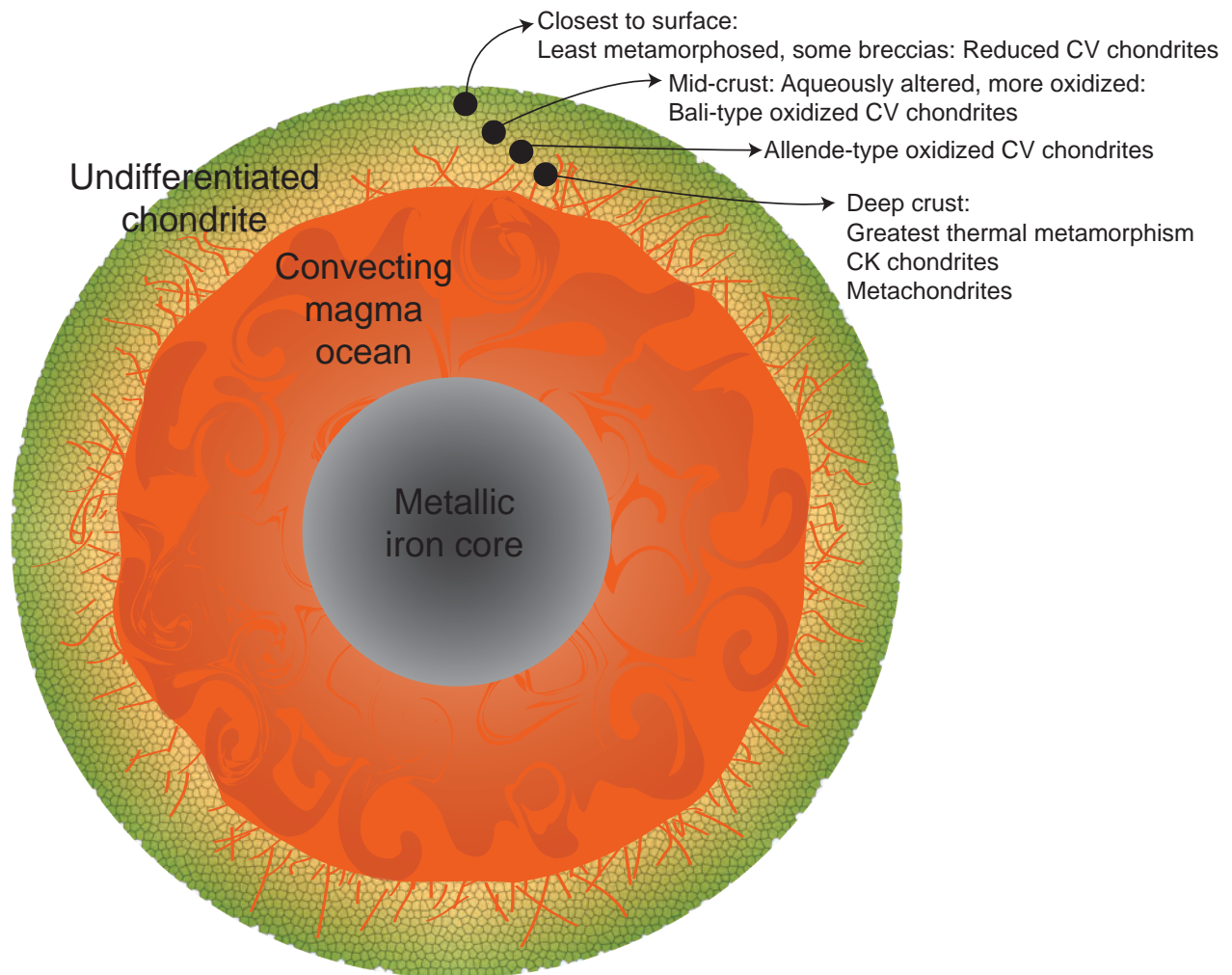
A. Ghosh, H.Y. McSween Jr., Temperature dependence of specific heat capacity and its effect on asteroid thermal models, Meteoritics and Planetary Science 34(1999) 121-127.

A. Ghosh, S.J. Weidenschilling, H.Y. McSween Jr., Importance of the accretion process in asteroid thermal evolution: 6 Hebe as an example, Meteoritics and Planetary Science 38(2003) 711-724.

J.D. Gilmour, C.A. Middleton, Anthropic selection of a Solar System with a high ^{26}Al/^{27}Al ratio: Implications and a possible mechanism, Icarus 201(2009) 821-823.

R.C. Greenwood, I.A. Franchi, A.T. Kearsley, O. Alard, The relationship between CK and CV chondrites, Geochemica et Cosmochimica Acta 74(2010) 1684-1705.

H. Haack, K.L. Rasmussen, P.H. Warren, Effects of regolith/megaregolith insulation on the cooling histories of differentiated asteroids., Journal of Geophysical Research 95(1990) 5111-5124.

P. Hevey, I. Sanders, A model for planetesimal meltdown by ^{26}Al and its implications for meteorite parent bodies, Meteoritics and Planetary Science 41(2006) 95-106.

C.M. Hohenberg, O.V. Pravdivtseva, A.P. Meshik, Trapped Xe and I-Xe ages in aqueously altered CV3 meteorites, Geochimica Et Cosmochimica Acta 68(2004) 4745-4763.

I. Hutcheon, K.K. Marhas, A.N. Krot, J.N. Goswami, R.H. Jones, ^{26}Al in plagioclase-rich chnodrules in carbonaceous chondrites: Evidence for an extended duration of chondrule formation, Geochimica Et Cosmochimica Acta 73(2009) 5080-5099.

A.J. Irving, T.E. Larson, F.J. Longstaffe, D. Rumble, T.E. Bunch, J.H. Wittke, S.M. Kuehner, A primitive achondrite with oxygen isotopic affinities to CV chondrites: Implications for differentiation and the size of the CV parent body, EOS Transactions of the American Geophysical Union 85(2004) P31C-02.

B. Jacobsen, Q. Yin, F. Moynier, Y. Amelin, A.N. Krot, ^{26}Al, ^{26}Mg and ^{207}Pb, ^{206}Pb systematics of Allende CAIs: Canonical solar initial ^{26}Al/^{27}Al ratio, Earth and Planetary Science Letters(2008).

H. Jeffreys, The Earth, Cambridge University Press, London, 1959.

A. Johansen, J.S. Oishi, M.-M. Mac Low, H. Klahr, T. Henning, A. Youdin, Rapid planetesimal formation in turbulent circumstellar disks, Nature 448(2007) 1022-1025.

V.C. Kress, I.S.E. Carmichael, The compressibility of silicate liquids containing Fe2O3 and the effect of composition, temperature, oxygen fugacity, and pressure on their redox states., Contributions to Mineralogy and Petrology 108(1991) 82-92.

A. Krot, E. Scott, M. Zolensky, Mineralogical and chemical modification of components in CV3 chondrites: Nebular or asteroidal processing, Meteoritics 30(1995).

A.N. Krot, M.I. Petaev, E.R.D. Scott, B.G. Choi, M.E. Zolensky, K. Keil, Progressive alteration in CV3 chondrites: More evidence for asteroidal alteration, Meteoritics and Planetary Science 33(1998) 1065-1085.

T. Kunihiro, A. Rubin, K. McKeegan, J. Wasson, Initial ^{26}Al/^{27}Al in carbonaceous-chondrite chondrules: too little ^{26}Al to melt asteroids, Geochimica Et Cosmochimica Acta 68(2004) 2947-2957.

R.A. Lange, I.S.E. Carmichael, TiO$_2$-SiO$_2$ liquids: New measurements and derived partial molar properties, Geochimica et Cosmochimica Acta 51(1987) 2931-2946.

T. Lee, D.A. Papanastassiou, G.J. Wasserburg, Demonstration of ^{25}Mg excess in Allende and evidence for ^{26}Al, Geophys. Res. Lett 3(1976) 41-44.

K. Lodders, B. Fegley, The Planetary Scientist's Companion, Oxford University Press, New York, 1998.

G.J. MacPherson, A.M. Davis, E.K. Zinner, The distribution of aluminum-26 in the early solar system: A reappraisal, Meteoritics and Planetary Science 30(1995) 365-386.

T.J. McCoy, D.W. Mittlefehldt, L. Wilson, Asteroid Differentiation, in: D.S.a.H.Y.M. Lauretta, (Ed), Meteorites and the Early Solar System II, University of Arizona Press, Tucson, 2006, pp. 733-745.

R. Merk, D. Breuer, T. Spohn, Numerical Modeling of ^{26}Al-Induced Radioactive Melting of Asteroids Considering Accretion, Icarus 159(2002) 183-191.

M. Miyamoto, N. Fujii, H. Takeda, Ordinary chondrite parent body: An internal heating model, Proceedings of the Lunar and Planetary Science Conference 12B(1981) 1145-1152.

B.J. Monaghan, P.N. Quested, Thermal diffusivity of iron at high temperature in both the liquid and solid states, Iron Steel Inst. Japan 41(2001) 1524-1528.

F. Nimmo, Energetics of asteroid dynamos and the role of compositional convection, Lunar and Planetary Science Conference XL(2009) 1142.

L.E. Nyquist, T. Kleine, C.-Y. Shih, Y.D. Reese, The distribution of short-lived radioisotopes in the early solar system and the chronology of asteroid accretion, differentiation, and secondary mineralization, Geochemica et Cosmochimica Acta 73(2009) 5115-5136.

C.P. Opeil, G.J. Consolmagno, D.T. Britt, The thermal conductivity of meteorites: New measurements and analysis, Icarus 208(2010) 449-454.

O.V. Pravdivtseva, A.N. Krot, C.M. Hohenberg, A.P. Meshik, M.K. Weisberg, K. Keil, The I-Xe record of alteration in the Allende CV chondrite, Geochimica Et Cosmochimica Acta 67(2003) 5011-5026.

S. Sahijpal, P. Soni, G. Gupta, Numerical simulations of the differentiation of accreting planetesimals with ^{26}Al and ^{60}Fe as the heat sources, Meteoritics &# 38; Planetary Science(2007).

B.E. Schmidt, P.C. Thomas, J.M. Bauer, J.-Y. Li, L.A. McFadden, M.J. Mutchler, S.C. Radcliffe, A.S. Rivkin, C.T. Russell, J.W. Parker, S.A. Stern, The shape and surface variation of 2 Pallas from the Hubble Space Telescope, Science 9(2009) 275-278.

M. Schölling, D. Breuer, Numerical simulation of convection in a partially molten planetesimal, European Planetary Science Congress 4, Potsdam, Germany, 2009, p. 523.

G. Schubert, K. Zhang, M.G. Kivelson, J.D. Anderson, The magnetic field and internal structure of Ganymede, Nature 384(1996) 544-545.

T.W. Sisson, T.L. Grove, Experimental investigations of the role of H2O in calc-alkaline differentiation and subduction zone magmatism, Contributions to Mineralogy and Petrology 113(1993) 143-166.

T. Swindle, Implications of I-Xe studies for the timing and location of secondary alteration, Meteoritics & Planetary Science 33(1998) 1147-1155.

G.J. Taylor, P. Maggiore, E. Scott, A. Rubin, K. Keil, Original structures, and fragmentation and reassembly histories of asteroids: Evidence from meteorites, Icarus 69(1987) 1-13.

P. Thomas, J. Parker, L. McFadden, C. Russell, S. Stern, M. Sykes, E. Young, Differentiation of the asteroid Ceres as revealed by its shape, Nature 437(2005) 224-226.

D.L. Turcotte, G. Schubert, Geodynamics, Cambridge University Press, Cambridge, 2002, 456 pp.

H.C. Urey, the cosmic abundances of potassium, uranium, and thorium and the heat balance of the Earth, the Moon, and Mars., Proceedings of the National Academy of Sciences 41(1955) 127-144.

P. Wasilewski, New magnetic results from Allende C3(V), Physics of the Earth and Planetary Interiors 26(1981) 134-148.

M.A. Weiczorek, M.T. Zuber, R.J. Phillips, The role of magma buoyancy on the eruption of lunar basalts, Earth and Planetary Science Letters 185(2001) 71-83.

B.P. Weiss, J.S. Berdahl, L. Elkins-Tanton, S. Stanley, E.A. Lima, L. Carporzen, Magnetism on the Angrite Parent Body and the Early Differentiation of Planetesimals, Science 322(2008) 713-716.

B.P. Weiss, L. Carporzen, L.T. Elkins-Tanton, D.L. Shuster, D.S. Ebel, J. Gattacceca, M.T. Zuber, J.H. Chen, D.A. Papanastassiou, R.P. Binzel, D. Rumble, A.J. Irving, A partially differentiated parent body for CV chondrites, Proceedings of the Lunar and Planetary Science Conference 41(2010) 1688.

Wilson L., K. Keil, the fate of pyroclasts produced in explosive eruptions on the asteroid 4 Vesta, Meteoritics and Planetary Science 32(1997) 813-823.

D.S. Woolum, P. Cassen, Astronomical constraints on nebular temperatures: Implications for planetesimal formation., Meteoritics and Planetary Science 34(1999) 897-907.

K. Yomogida, T. Matsui, Multiple parent bodies of ordinary chondrites, Earth and Planetary Science Letters 68(1984) 34-42.

E. Young, K. Zhang, G. Schubert, Conditions for pore water convection within carbonaceous chondrite parent bodies: Implications for planetesimal size and heat production, Earth and Planetary Science Letters 213(2003) 249-259.

Closest to surface:
Least metamorphosed, some breccias: Reduced CV chondrites

Mid-crust: Aqueously altered, more oxidized:
Bali-type oxidized CV chondrites

Allende-type oxidized CV chondrites

Deep crust:
Greatest thermal metamorphism
CK chondrites
Metachondrites

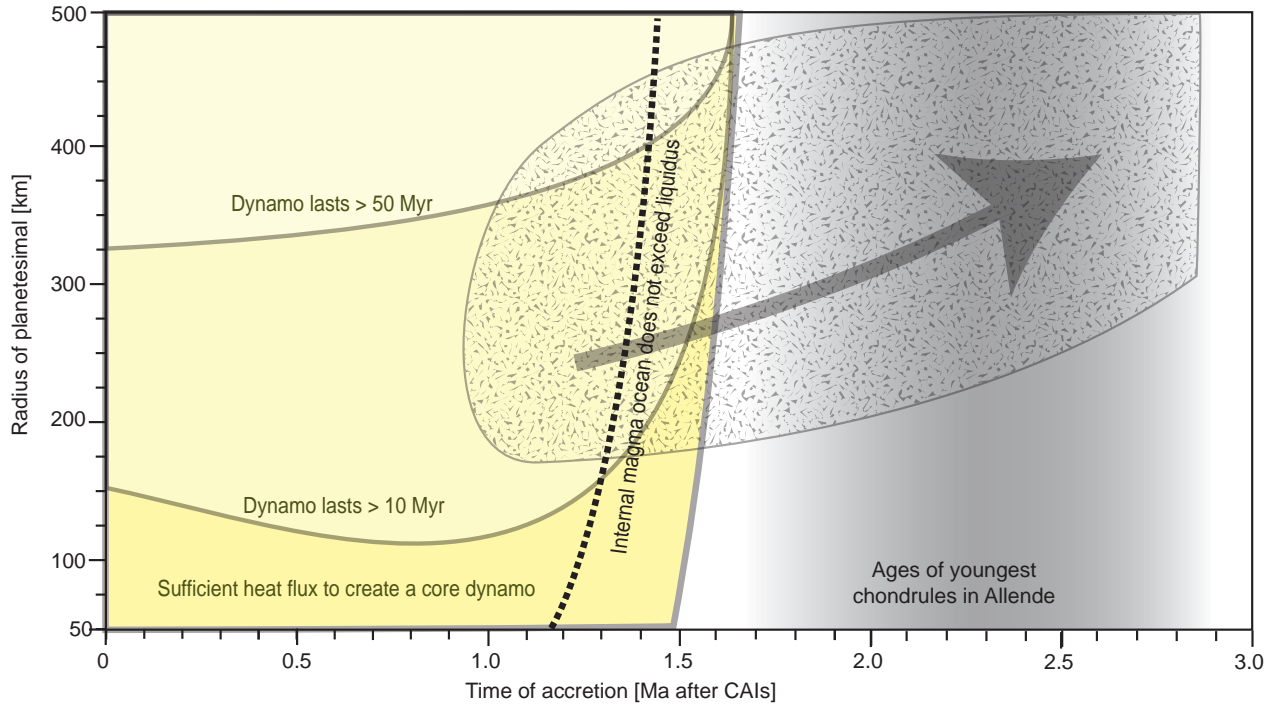Undifferentiated chondrite

Convecting magma ocean

Metallic iron core

2

3   **Figure 1.** Schematic diagram of proposed structure for the CV parent body, including an iron core,

4   internal magma ocean, and undifferentiated chondritic crust with varying levels of metamorphism

5   and metasomatism.

6
7

Figure 2. Summary of model results for the CV chondrite parent body and predictions for its size and

thermal history. Bodies with sufficient heat flux to create a core dynamo assuming instantaneous

accretion are shown in yellow. Additional contours are given showing the longevity of the

resulting core dynamo. The ages of the youngest chondrules in Allende are shown in the vertical

grey band. Constraints from Allende indicate that its parent body had a long-lived magnetic field

(lasting until at least 10 Ma after CAIs), and a thick unmelted crust. Accretion over a period of

time is therefore required. We suggest a path of accretion that lies in the patterned area; the arrow

is an example path. Earlier accretion to a given radius produces a body with such a thin crust that

foundering is likely. The body must accrete closer to 1 Ma, so that internal temperatures do not rise

too high, and then continue accreting material to the crust while the core dynamo continues.

1
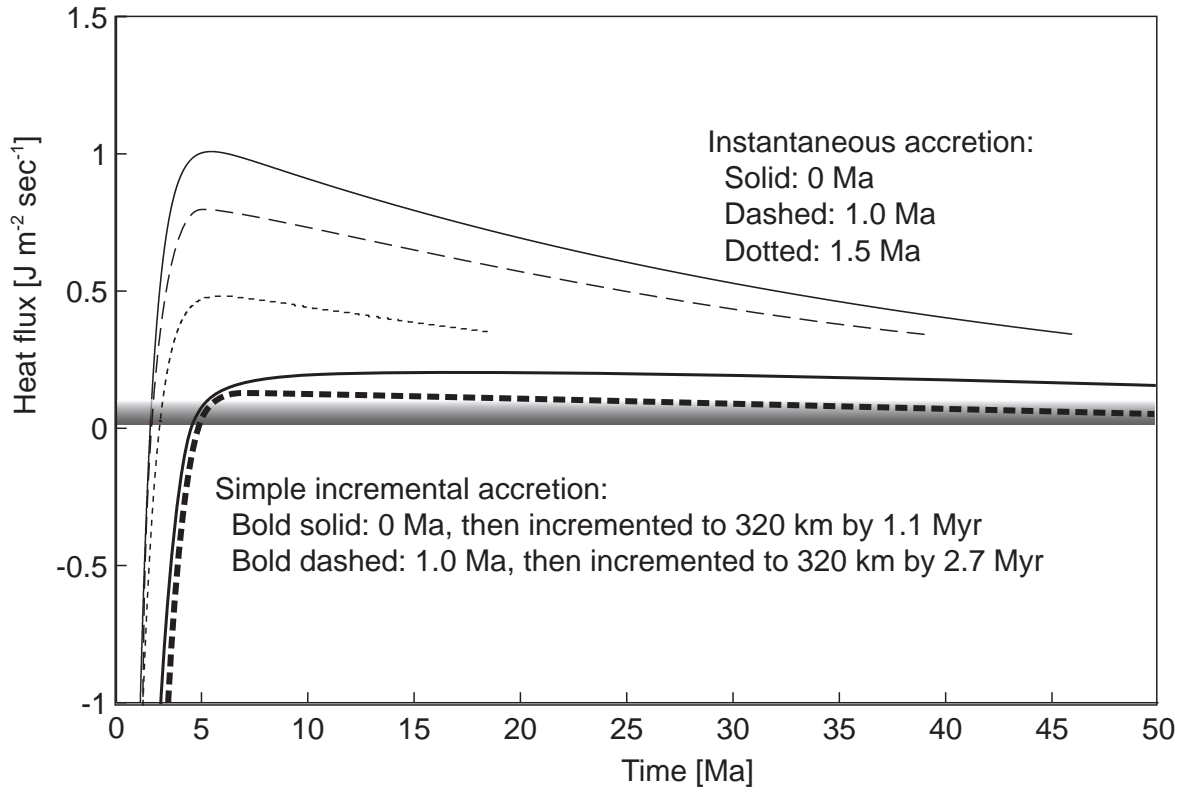
Figure 3. Core heat flux from planetesimals as a function of time after CAIs formation. Planetesimals

with radius 300 km are shown at three ages of instantaneous accretion: 0, 1.0, and 1.5 Ma after

CAI formation. Two additional models are shown with instantaneous accretion at 0 and 1.0 Ma

after CAIs, followed by regular increments of cold material to the planetesimal surface until the

total radius equals 320 km. The shaded region at bottom marks the heat fluxes that must be

exceeded for the production of a core dynamo. When internal temperatures fall below 1,000°C

convection is assumed to cease and the calculations are terminated.

2

3

4

5

6

7

8

9

10

11
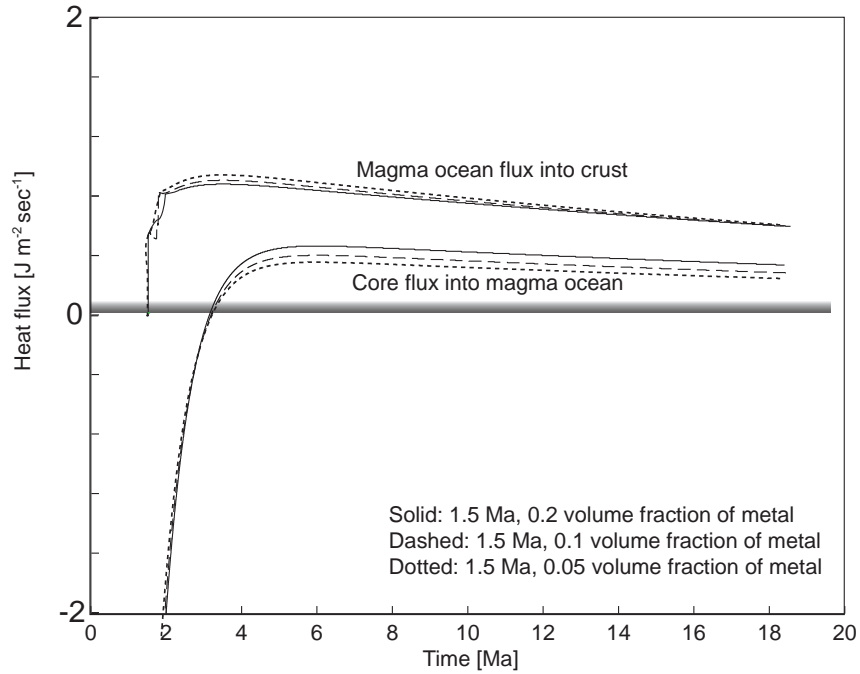
Figure 4: Magma ocean and core heat fluxes for 300-km-radius bodies accreted instantaneously at 1.5 Ma after CAI formation as a function of the volume fraction of Fe metal in the body. The core heat fluxes are comparable for bulk metal contents of 0.05, 0.1, and 0.2 volume fractions. All bodies melt to within 10 km of the surface. The radii of the final cores produced through metal segregation at every melting increment are 108 km, 137 km, and 172 km, respectively.

1
2

3
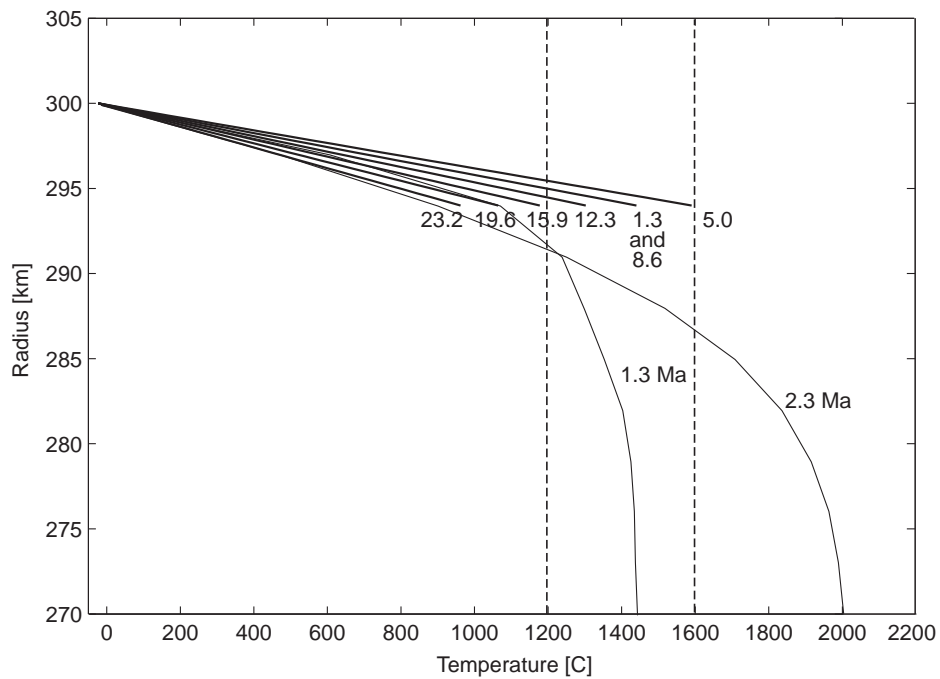
Figure 5: Temperature profiles for a body with radius 300 km that accreted instantaneously at 1.0 Ma

after CAI formation. Dashed lines: solidus and liquidus. Two thin lines, from Equation 2:

temperature profile at 1.3 Ma, passed to the convective code, and a later profile at 2.3 Ma,

included for comparison. Bold lines: profiles from the conductive lid overlying a homogeneously

mixed internal magma ocean at the temperature of the bottom of the lid, at 1.3, 5.0, 8.6 12.3, 15.9,

19.6, and 23.2 Ma. The temperatures at the bottom three nodes of the conductive lid at 5.0 Ma

exceed our stated lid temperature of 1400ºC, but the lid is constrained in the code to be no thinner

than 2% of the planetesimal radius, or in this case, 6 km. The 6 km limit was reached immediately

at 1.3 Ma and retained afterward. Note that the solution to equation (2) at 2.3 Ma gives a lid under

1400ºC that is ~10 km thick, rather than the ~6 km thickness from this code; allowing the interior

to be convectively well-mixed removes the curving boundary layer.
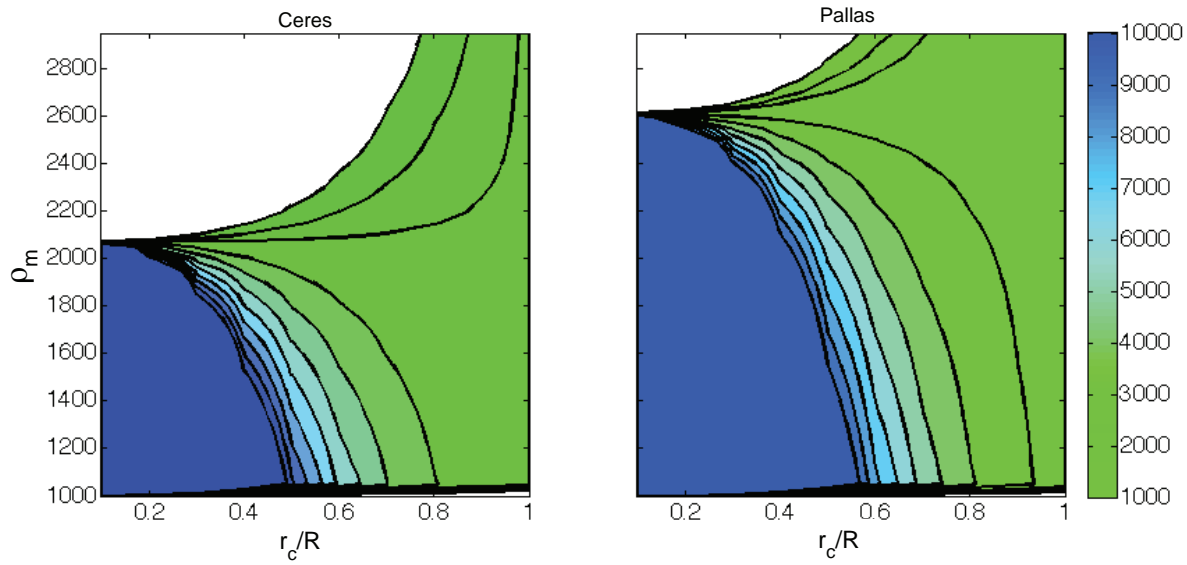
1
2
3

4   **Figure 6.** Contours of core density (ρ_c) for core radius/planetary radius (r_c/R) and mantle density (ρ_m)

5   for 1 Ceres (left) and 2 Pallas (right). Core densities in the range of iron metal but as light as pure

6   silicate are consistent with observations. Both bodies have mantle densities consistent with an ice

7   and silicate mixture.

8
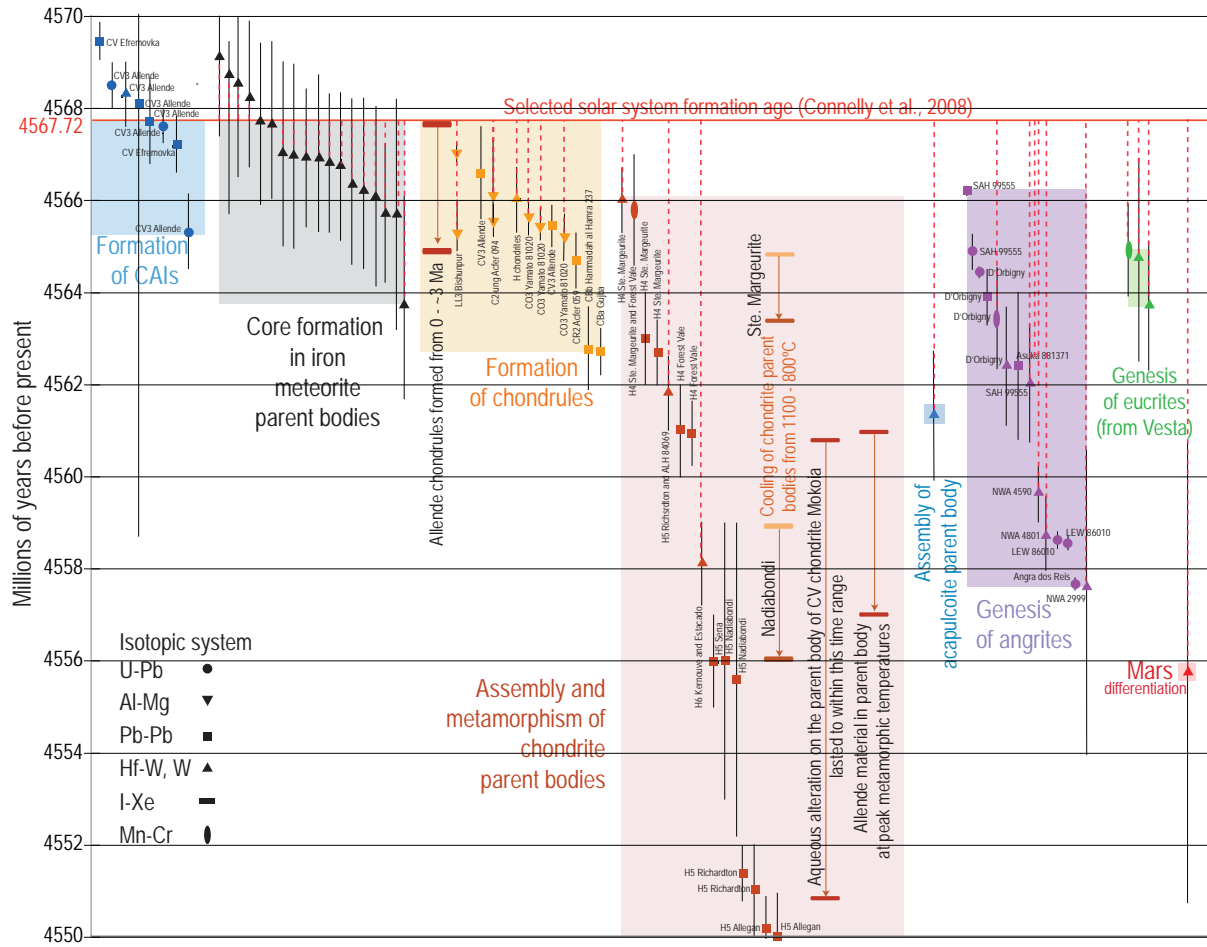
1
2 **Figure 7**. Age constraints on meteorite and parent body evolution. Red dashed lines indicate ages

3 calculated relative to the selected age of oldest CAI. The early ages of CV chondrite chondrules

4 and CV meteorite evidence for relatively protracted thermal metamorphism indicate an early

5 accretion age for the CV parent body. All dates and references in Table SD1.

6

1

2
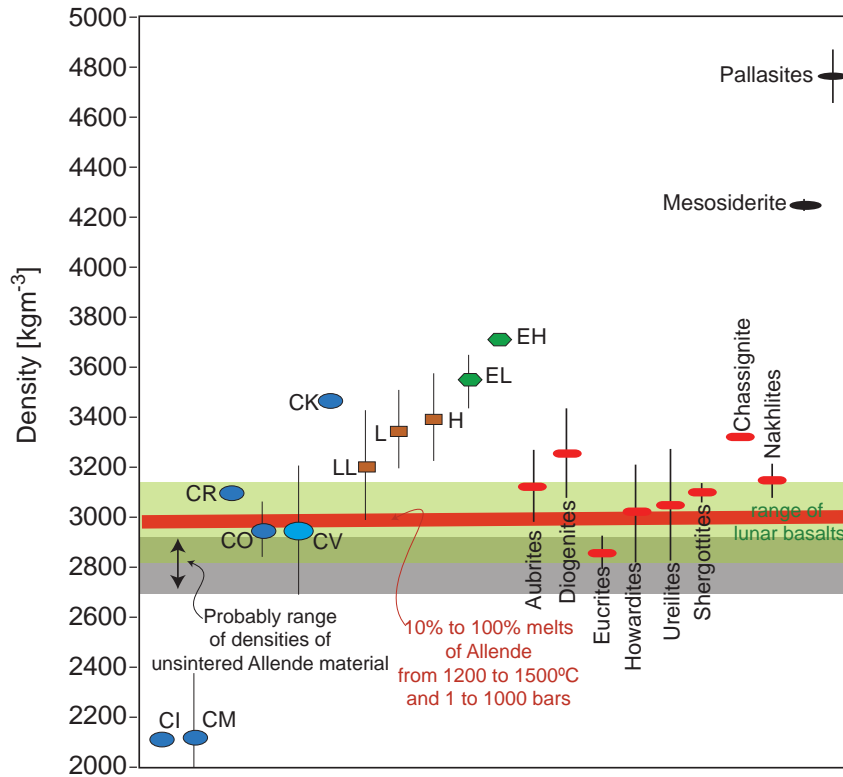
Figure 8. Densities of materials that would be found in the modelled differentiated planetesimals, and various other solar system materials for comparison. Densities of carbonaceous and ordinary chondrites, achondrites, and iron meteorites from Britt and Consolmagno (2003). Range of lunar basalt densities from Wieczorek et al. (2001). Allende melt densities calculated as described in text.

1   TABLES

2   Table 1: Parameters used in models.

Variable	Symbol	Value(s)	Units	Ref.
Initial and surface temperature	T_0	250	K	(Woolum and Cassen 1999)
Planetesimal radius	r	50,000, 100,000, 200,000, 300,000, 400,000, 500,000	m	
Age of instantaneous accretion		0, 1, 1.5	Ma after CAI formation	
Metal in bulk starting material (for core formation)		0.05, 0.1, 0.2	Volume fraction	
Density of conductive lid	ρ_{LID}	2,900	kg m^{-3}	(Britt and Consolmagno 2003)
Density of planetesimal magma ocean	ρ_{MO}	3,000	kg m^{-3}	
Density of iron core	ρ_{CORE}	8,000	kg m^{-3}	
Thermal diffusivity of crust	κ	8×10^{-7}	m^2 s^{-1}	(Opeil et al. 2010)
Thermal diffusivity of core	κ	6×10^{-5}	m^2 s^{-1}	(Monaghan and Quested 2001)
Thermal conductivity of conductive lid	K_{LID}	1.5	W m^{-1} K^{-1}	(Opeil et al. 2010)
Thermal conductivity	K	2.1	W m^{-1} K^{-1}	
Heat capacity of silicates	C_P	800	J kg^{-1} K^{-1}	(Fabrichnaya 1999, Ghosh and McSween Jr. 1999)
Heat capacity of iron core	C_{P_CORE}	850	J kg^{-1} K^{-1}	(Bartels and Grove 1991)
Heat of fusion of silicates	H_f	400,000	J kg^{-1}	(Ghosh and McSween Jr. 1998)
Heating production of ^{26}Al decay	H_0	0.355	W kg^{26}Al^{-1}	(Castillo-Rogez et al. 2009)
Aluminum content of CV chondrites	X_{Al}	1.8	wt%	(Lodders and Fegley 1998)
Initial ^{26}Al/^{27}Al ratio	$^{26}Al_0$	5×10^{-5}		(Lee et al. 1976, MacPherson et al. 1995)
Fraction of ^{26}Al in bulk material	C_0	$^{26}Al_0\ X_{Al}$		
Decay constant	λ	3.0124×10^{-14}	s^{-1}	(Castillo-Rogez et al. 2009)

3